A 50-Gb/s 10-mW Analog Equalizer Using Transformer Feedback Technique in 65-nm CMOS Technology

Jian-Hao Lu and Shen-Iuan Liu, *Senior Member, IEEE*

***Abstract*—A 50-Gb/s low-power analog equalizer has been realized in 65-nm CMOS technology. This equalizer adopts the proposed transformer feedback technique to achieve a peaking gain of 18 dB at 25 GHz and low-power dissipation. The whole equalizer without the output buffer consumes 10 mW from a 1-V supply. The chip occupies 0.35×0.27 mm^2. For a 50-Gb/s pseudorandom bit sequence of $2^7 - 1$, the measured bit error rate is less than 10^{-12}, and the measured maximum root-mean-square and peak-to-peak jitters are 2.7 and 12.4 ps, respectively.**

***Index Terms*—CMOS, equalizer, transformer feedback.**

I. Introduction

DUE to frequency-dependent impairments such as skin effect and dielectric loss, high-speed data transmission suffers from severe intersymbol interference (ISI). To eliminate the ISI and improve the bit error rate (BER), high-speed equalizers [1]–[9] have been used widely in modern broadband data communications. Although a 49-Gb/s transversal filter has been realized in 0.18-μm SiGe BiCMOS technology (with an f_{T} of 160 GHz) for equalization [1], the power dissipation of 750 mW makes the applications difficult. However, CMOS equalizers [2]–[7] and other BiCMOS equalizers [8], [9] have been demonstrated up to only 10–40 Gb/s. As a result, it is highly desirable to develop a high-speed and low-power equalizer, particularly in CMOS technology.

Unlike the constant feedback factor in a conventional resistive feedback amplifier, the proposed transformer feedback amplifier further extends the bandwidth by reducing the feedback factor at high frequencies. Compared with the active feedback amplifier [2], [10], this transformer feedback amplifier achieves both a wide bandwidth and low-power dissipation. In this work, a 50-Gb/s 10-mW CMOS equalizer is realized by using the proposed transformer feedback amplifier.

II. Equalizer Design

Fig. 1(a) shows the measured loss for a typical copper cable. This cable loss becomes larger at higher frequencies, and it reaches 18 dB at 25 GHz. To compensate the cable loss, a 50-Gb/s low-power analog equalizer is proposed, as shown in Fig. 1(b). This equalizer consists of the proposed transformer feedback amplifier, a predriver, and an output buffer. The transformer feedback amplifier realizes a peaking gain of 18 dB at 25 GHz, while the predriver is composed of two stages, with each stage exhibiting a bandwidth of 30 GHz. The detailed circuits are discussed as follows.

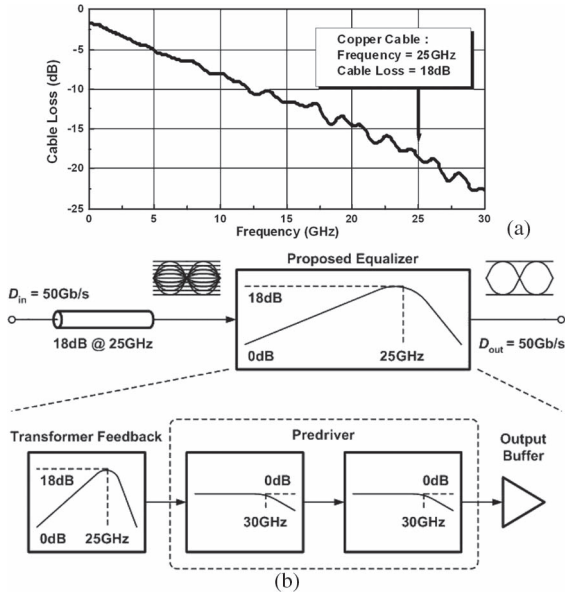

Fig. 1. (a) Measured loss for a typical copper cable. (b) Proposed 50-Gb/s low-power analog equalizer.

A. Transformer Feedback Amplifier

Fig. 2 shows the proposed transformer feedback amplifier, where the transformer is composed of the feedback inductance L_f and the gate inductance L_g with their mutual inductance M. In general, the mutual inductance is a function of the geometric mean of the two individual inductances, and it is expressed as

$$M = k\sqrt{L_f L_g} \tag{1}$$

where k denotes the coupling coefficient. Note that the coupling coefficient is a strong function of the physical arrangement. Here, R_d and C_d represent the output load resistance and the parasitic capacitance at the drain, respectively, while R_f denotes the feedback resistance of this amplifier. To quantitatively analyze the proposed transformer feedback amplifier, its

Manuscript received February 7, 2009; revised May 15, 2009 and August 10, 2009. Current version published October 16, 2009. This work was supported by the National Science Council (NSC). This paper was recommended by Associate Editor Y. Chiu.

The authors are with the Graduate Institute of Electronics Engineering and Department of Electrical Engineering, National Taiwan University, Taipei 10617, Taiwan (e-mail: lsi@cc.ee.ntu.edu.tw).

Color versions of one or more of the figures in this paper are available online at http://ieeexplore.ieee.org.

Digital Object Identifier 10.1109/TCSII.2009.2030536

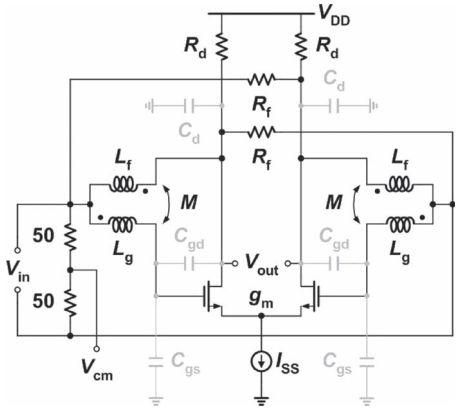

Fig. 2. Proposed transformer feedback amplifier.

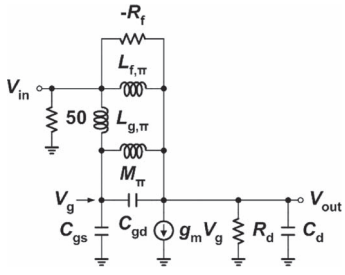

Fig. 3. Small-signal equivalent half-circuit of the proposed transformer feedback amplifier.

small-signal equivalent half-circuit is shown in Fig. 3, where the transformer is replaced by its equivalent π network with the following three relationships:

$$L_{f,\pi} = \frac{L_f L_g - M^2}{L_g + M} \tag{2}$$

$$L_{g,\pi} = \frac{L_f L_g - M^2}{L_f + M} \tag{3}$$

$$M_\pi = \frac{L_f L_g - M^2}{-M}. \tag{4}$$

By applying Kirchhoff's current law (KCL) at the nodes V_g and $V_{\rm out}$, we, respectively, get the two following equations:

$$\frac{V_{\rm in} - V_g}{sL_{g,\pi}} = V_g \times sC_{gs} + (V_g - V_{\rm out}) \times sC_{gd} + \frac{V_g - V_{\rm out}}{sM_\pi} \tag{5}$$

$$(V_g - V_{\rm out}) \times sC_{gd} + \frac{V_g - V_{\rm out}}{sM_\pi} + \frac{V_{\rm in} - V_{\rm out}}{sL_{f,\pi}} + \frac{V_{\rm in} - V_{\rm out}}{-R_f} = g_m V_g + \frac{V_{\rm out}}{R_d} + V_{\rm out} \times sC_d. \tag{6}$$

Here, C_{gd} and C_{gs} represent the gate-drain and the gate-source parasitic capacitances, respectively, while g_m denotes the transconductance of this transformer feedback amplifier. According to (5) and (6), the transfer function of the proposed transformer feedback amplifier is derived as

$$\frac{V_{\rm out}}{V_{\rm in}}(s) = \frac{a_0 + a_1 s + a_2 s^2 + a_3 s^3}{b_0 + b_1 s + b_2 s^2 + b_3 s^3 + b_4 s^4} \equiv \frac{N(s)}{D(s)} \tag{7}$$

where the numerator and the denominator are denoted by $N(s)$ and $D(s)$, respectively. Their polynomial coefficients are given in the Appendix. Note that a_0 equals b_0, and it indicates that the low-frequency gain is unity (0 dB). This is because the input and output of the transformer feedback amplifier are short-circuited by the feedback inductance L_f at dc. This architecture exactly meets the low-frequency cable losses. In conventional equalizers, however, the unity low-frequency gain is achieved by additional capacitive and resistive source degenerations, which results in more power dissipation.

Although the numerator is a third-order polynomial, it can approximately be rewritten as

$$N(s) \approx a_1(s - \omega_{z1}) \tag{8}$$

if $\omega_{z1} \ll \omega_{z2}$ and ω_{z3}, where ω_{z1} denotes the dominant zero, and ω_{z2} and ω_{z3} denote other nondominant zeros. Here, ω_{z1} is given by

$$\omega_{z1} = \frac{R_f(L_{f,\pi} + L_{g,\pi} + M_\pi)}{L_{f,\pi}(L_{g,\pi} + M_\pi + g_m R_f M_\pi)}. \tag{9}$$

Similarly, the denominator of a fourth-order polynomial can be approximated as a second-order one as

$$D(s) \approx b_2\left(s^2 + 2\zeta\omega_n s + \omega_n^2\right) \tag{10}$$

if $\omega_{p1,2} \ll \omega_{p3,4}$, where $\omega_{p1,2}$ and $\omega_{p3,4}$ denote the complex dominant and nondominant poles, respectively. Here, ζ and ω_n are given by (11) and (12), shown at the bottom of the next page. By applying the following three lemmas:

$$\frac{L_{f,\pi} M_\pi}{L_{f,\pi} + L_{g,\pi} + M_\pi} = L_f + M \tag{13}$$

$$\frac{L_{g,\pi} M_\pi}{L_{f,\pi} + L_{g,\pi} + M_\pi} = L_g + M \tag{14}$$

$$\frac{L_{f,\pi} L_{g,\pi}}{L_{f,\pi} + L_{g,\pi} + M_\pi} = -M \tag{15}$$

which are judiciously manipulated from (2)–(4), (9), (11), and (12) are correspondingly rewritten as

$$\omega_{z1} = \frac{R_f}{L_f + g_m R_f(L_f + M)} \tag{16}$$

$$\zeta = \frac{R_f(L_f - g_m R_d M) - R_d L_f}{2R_d R_f \sqrt{L_f(C_d + C_{gd}) + L_g(C_{gd} + C_{gs}) + 2MC_{gd}}} \tag{17}$$

$$\omega_n = \sqrt{\frac{1}{L_f(C_d + C_{gd}) + L_g(C_{gd} + C_{gs}) + 2MC_{gd}}}. \tag{18}$$

To give more insights, the discussion is divided into four situations.

1) Equations (16)–(18) are simplified, by letting $R_f = \infty$ and $M = 0$, as

$$\omega_{z1} = \frac{1}{g_m L_f} \tag{19}$$

$$\zeta = \frac{L_f}{2R_d \sqrt{L_f(C_d + C_{gd}) + L_g(C_{gd} + C_{gs})}} \tag{20}$$

$$\omega_n = \sqrt{\frac{1}{L_f(C_d + C_{gd}) + L_g(C_{gd} + C_{gs})}} \tag{21}$$

i.e., only the feedback inductance L_f and the gate inductance L_g of the feedback transformer are taken into consideration. Since the peaking gain of this transformer feedback amplifier is partially contributed by the dominant zero ω_{z1}, it should be designed to be as low as possible so that the peaking gain resulting from the dominant zero itself is maximum. From (19), it is found that g_m and L_f should be chosen to be large enough to achieve a lower ω_{z1}. To achieve a lower ω_{z1} and consequently increase the peaking gain contributed by the dominant zero, g_m and L_f are chosen to be as large as 22 mA/V and 625 pH, respectively. However, from (20), the large L_f leads to $\zeta > 0.707$. Thus, there is no additional peaking gain resulting from the complex dominant poles $\omega_{p1,2}$. To obtain an additional peaking gain contributed by the complex dominant poles without sacrificing that resulting from the dominant zero, the feedback resistance R_f and the mutual inductance M of the feedback transformer are introduced.

2) For the case where only R_f is considered, (16)–(18) are degenerated, by letting $M = 0$, to

$$\omega_{z1} = \frac{R_f}{L_f(1 + g_m R_f)} \tag{22}$$

$$\zeta = \frac{L_f(R_f - R_d)}{2R_d R_f \sqrt{L_f(C_d + C_{gd}) + L_g(C_{gd} + C_{gs})}} \tag{23}$$

and (21). If (19) and (20) are compared with (22) and (23), it is found that R_f reduces both ω_{z1} and ζ. To achieve $\zeta < 0.707$ and consequently obtain an additional peaking gain contributed by the complex dominant poles $\omega_{p1,2}$, R_f is chosen to be 186 Ω, resulting in $\zeta = 0.557$. Therefore, additional peaking gains of 1.6 and 3.5 dB, shown in Fig. 4(a) and (b), are increased by the dominant zero and the complex dominant poles at 25 GHz, respectively.

3) Similarly, for the case where only M is considered, (16) and (17) are degenerated, by letting $R_f = \infty$, to

$$\omega_{z1} = \frac{1}{g_m(L_f + M)} \tag{24}$$

$$\zeta = \frac{L_f - g_m R_d M}{2R_d \sqrt{L_f(C_d + C_{gd}) + L_g(C_{gd} + C_{gs}) + 2MC_{gd}}} \tag{25}$$

while (18) still holds. If (19) and (20) are compared with (24) and (25), it is found that M also reduces both ω_{z1} and ζ. To again obtain an additional peaking gain contributed by the complex dominant poles $\omega_{p1,2}$, M is chosen to be 180 pH, resulting in $\zeta = 0.487$. Therefore, additional peaking gains of 1.9 and 4.4 dB, shown in Fig. 4(a) and (b), are increased by the dominant zero and the complex dominant poles at 25 GHz, respectively.

4) Finally, for the case where both R_f and M are considered, both ω_{z1} and ζ are significantly reduced if (19) and (20) are compared with (16) and (17). It is found that the peaking gains of 10.7, 7.3, and 18 dB shown in Fig. 4(a)–(c) are realized by the dominant zero, the

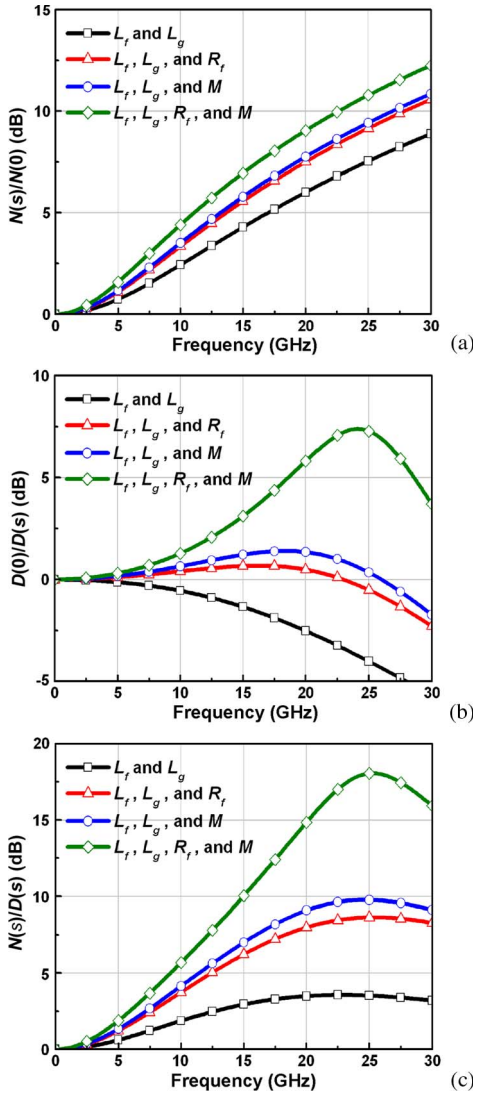

Fig. 4. Simulated frequency response of the transformer feedback amplifier for (a) only the normalized numerator $N(s)/N(0)$, (b) only the normalized denominator $D(0)/D(s)$, and (c) the overall transfer function $N(s)/D(s)$.

$$\zeta = \frac{L_{f,\pi}\left[R_f(L_{g,\pi} + g_m R_d L_{g,\pi} + M_\pi) - R_d(L_{g,\pi} + M_\pi)\right]}{2R_d R_f \sqrt{(L_{f,\pi} + L_{g,\pi} + M_\pi)\left[L_{f,\pi}L_{g,\pi}(C_d + C_{gs}) + L_{f,\pi}M_\pi(C_d + C_{gd}) + L_{g,\pi}M_\pi(C_{gd} + C_{gs})\right]}} \tag{11}$$

$$\omega_n = \sqrt{\frac{L_{f,\pi} + L_{g,\pi} + M_\pi}{L_{f,\pi}L_{g,\pi}(C_d + C_{gs}) + L_{f,\pi}M_\pi(C_d + C_{gd}) + L_{g,\pi}M_\pi(C_{gd} + C_{gs})}} \tag{12}$$

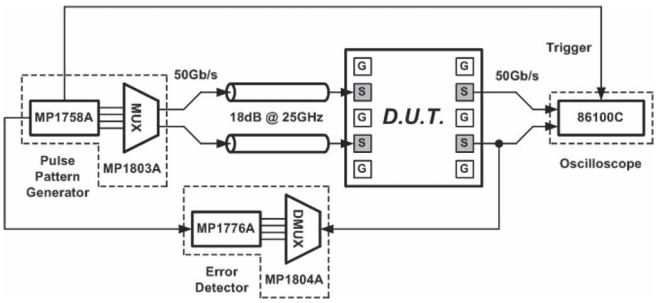

Fig. 5. Testing setup.

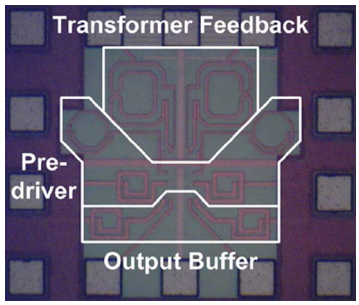

Fig. 6. Die photo.

complex dominant poles, and both of them combined at 25 GHz, respectively. However, the complex dominant poles with a large peaking gain may induce an issue of stability. For a stable feedback system, all poles should be located in the left half-plane. In other words, ζ must be positive. From (17), there exist a minimum of R_f given by

$$R_f > \frac{R_d L_f}{L_f - g_m R_d M} \tag{26}$$

or a maximum of M given by

$$M < \frac{L_f(R_f - R_d)}{g_m R_d R_f}. \tag{27}$$

In this work, ζ is finally designed to be 0.219.

According to the simulation results, the peaking gain is more sensitive to R_d, while the peaking frequency is more sensitive to L_f in comparison with other designed parameters.

B. Predriver and Output Buffer

To drive the output buffer, a two-stage predriver is realized by a shunt inductive-peaking technique where each stage exhibits a bandwidth of 30 GHz. Similarly, the output buffer also adopts the shunt inductive-peaking technique to extend the bandwidth.

III. Experimental Results

This equalizer has been fabricated in 65-nm CMOS technology and tested on a high-speed probe station with ground-signal-ground-signal-ground probes. Fig. 5 shows the testing setup. A 50-Gb/s pseudorandom bit sequence (PRBS) is provided by an Anritsu pulse pattern generator (MP1758A and

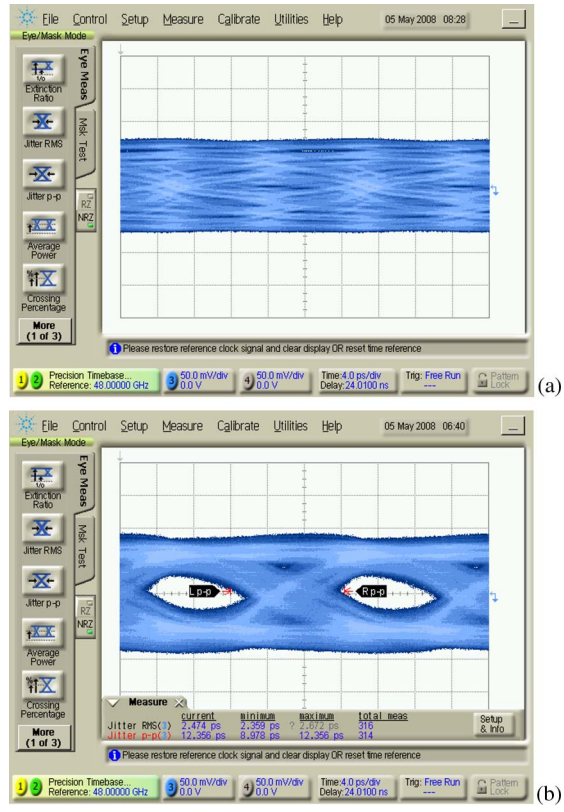

Fig. 7. Measured waveforms (a) before and (b) after the equalizer for a cable loss of 18 dB with a 50-Gb/s PRBS of $2^7 - 1$ (horizontal scale: 4 ps/div, vertical scale: 50 mV/div).

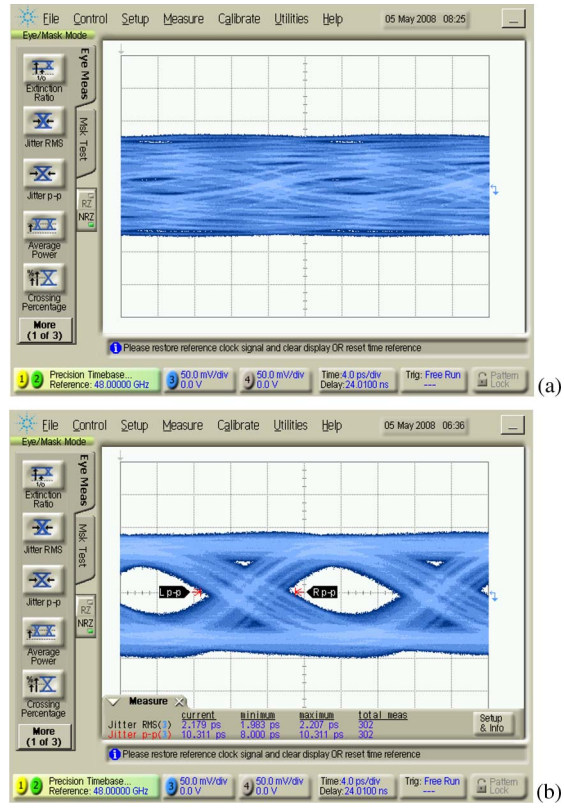

Fig. 8. Measured waveforms (a) before and (b) after the equalizer for a cable loss of 17 dB with a 48-Gb/s PRBS of $2^7 - 1$ (horizontal scale: 4 ps/div, vertical scale: 50 mV/div).

TABLE I
PERFORMANCE SUMMARY

	[3]	[4]	[5]	[6]	This Work
CMOS Tech.	0.13μm	0.13μm	90nm	0.13μm	65nm
Data Rate	10Gb/s	20Gb/s	30Gb/s	40Gb/s	50Gb/s
Peaking Gain	20dB @ 5GHz	15dB @ 10GHz	14.4dB @ 15GHz	14dB @ 20GHz	18dB @ 25GHz
Jitter	$20ps_{pp}$ (2^7-1)	$14ps_{pp}$ (2^{31}-1)	N/A (2^{31}-1)	$12.6ps_{pp}$ (2^7-1)	$2.2ps_{rms}$; $10.3ps_{pp}$ (48Gb/s, 2^7-1) $2.7ps_{rms}$; $12.4ps_{pp}$ (50Gb/s, 2^7-1)
Output Swing	$600mV_{pp}$	$300mV_{pp}$	$30mV_{pp}$	$400mV_{pp}$	$400mV_{pp}$
BER	N/A	$< 10^{-15}$	N/A	$< 10^{-12}$	$< 10^{-12}$
Chip Area	$0.162mm^2$	$0.2mm^2$	$0.3mm^2$	$0.25mm^2$	$0.095mm^2$
Power Diss.	25mW	60mW	25mW	14.4mW	10mW
Supply	1.2V	1.5V	1V	1.2V	1V

MP1803A) and subjected to a cable loss of 18 dB at 25 GHz. These attenuated data are equalized by the proposed equalizer. Then, the measured waveforms are displayed on an Agilent oscilloscope (86100C) and tested by an Anritsu error detector (MP1776A and MP1804A) for the BER testing. Fig. 6 shows the die photo, and it occupies 0.35×0.27 mm^2. This equalizer consists of a transformer feedback amplifier, a predriver, and an output buffer. Two on-chip 50-Ω resistors are applied to the termination and the common-mode voltage of the differential input.

The measured waveforms before and after the equalizer for cable losses of 18 dB with a 50-Gb/s PRBS of $2^7 - 1$ and 17 dB with a 48-Gb/s PRBS of $2^7 - 1$ are shown in Figs. 7(a) and (b) and 8(a) and (b), respectively. For data rates up to 50 Gb/s, the eye is fully closed before equalization. After equalization, the received data are successfully equalized, and the maximum root-mean-square (rms) peak-to-peak jitters for a 50-Gb/s PRBS of $2^7 - 1$ are measured as 2.7 and 12.4 ps, respectively, where the intrinsic rms and peak-to-peak jitters of 748 fs and 4.4 ps are generated by the pulse pattern generator itself. The peaking gain of 7.3 dB resulting from the complex dominant poles $\omega_{p1,2}$ may be too large, leading to substantial phase distortions. Since the maximum trigger frequency of an Agilent precision timebase reference module (86107A) is up to only 48 GHz, the measured waveforms will suffer from another intrinsic jitter generated by the oscilloscope beyond this frequency. Therefore, the maximum rms and peak-to-peak jitters for a 48-Gb/s PRBS of $2^7 - 1$ are also measured as 2.2 and 10.3 ps, respectively, with the intrinsic rms and peak-to-peak jitters of 609 fs and 3.4 ps. The output swing is 400 mV_{pp}, and the measured BER is less than 10^{-12} in response to a 50-Gb/s PRBS of $2^7 - 1$. This equalizer without the output buffer consumes 10 mW from a 1-V supply, of which 4 mW is dissipated in the transformer feedback amplifier and 6 mW is dissipated in the predriver. Table I summarizes the performance of the proposed equalizer along with those of previous works.

IV. CONCLUSION

A 50-Gb/s 10-mW analog equalizer has been realized in 65-nm CMOS technology. By using the proposed transformer feedback technique, the equalizer achieves a peaking gain of 18 dB at 25 GHz. This chip occupies 0.35×0.27 mm^2. The measured maximum peak-to-peak jitters for a 50-Gb/s PRBS of $2^7 - 1$ and a 48-Gb/s PRBS of $2^7 - 1$ are 12.4 and 10.3 ps, respectively. The output swing is 400 mV_{pp}, and the measured BER is less than 10^{-12} in response to a 50-Gb/s PRBS of $2^7 - 1$.

APPENDIX

The polynomial coefficients of the transfer function of the proposed transformer feedback amplifier are expressed as

$$a_0 = b_0 = R_d R_f (L_{f,\pi} + L_{g,\pi} + M_\pi) \tag{28}$$
$$a_1 = -R_d L_{f,\pi} (L_{g,\pi} + M_\pi + g_m R_f M_\pi) \tag{29}$$
$$a_2 = R_d R_f M_\pi (L_{f,\pi} C_{gd} + L_{g,\pi} C_{gd} + L_{g,\pi} C_{gs}) \tag{30}$$
$$a_3 = -R_d L_{f,\pi} L_{g,\pi} M_\pi (C_{gd} + C_{gs}) \tag{31}$$
$$b_1 = L_{f,\pi} [R_f (L_{g,\pi} + g_m R_d L_{g,\pi} + M_\pi) - R_d (L_{g,\pi} + M_\pi)] \tag{32}$$
$$b_2 = R_d R_f [L_{f,\pi} L_{g,\pi} (C_d + C_{gs}) + L_{f,\pi} M_\pi (C_d + C_{gd}) + L_{g,\pi} M_\pi (C_{gd} + C_{gs})] \tag{33}$$
$$b_3 = L_{f,\pi} L_{g,\pi} M_\pi [R_f (C_{gd} + g_m R_d C_{gd} + C_{gs}) - R_d (C_{gd} + C_{gs})] \tag{34}$$
$$b_4 = R_d R_f L_{f,\pi} L_{g,\pi} M_\pi (C_d C_{gd} + C_d C_{gs} + C_{gd} C_{gs}). \tag{35}$$

ACKNOWLEDGMENT

The authors would like to thank the Taiwan Semiconductor Manufacturing Company for the chip fabrication.

REFERENCES

[1] A. Hazneci and S. P. Voinigescu, "A 49-Gb/s, 7-tap transversal filter in 0.18 μm SiGe BiCMOS for backplane equalization," in *IEEE Compound Semicond. Integr. Circuit Symp.*, Oct. 2004, pp. 101–104.

[2] Y. Tomita, M. Kibune, J. Ogawa, W. W. Walker, H. Tamura, and T. Kuroda, "A 10 Gb/s receiver with equalizer and on-chip ISI monitor in 0.11 μm CMOS," in *IEEE Symp. VLSI Circuits Dig. Tech. Papers*, Jun. 2004, pp. 202–205.

[3] S. Gondi, J. Lee, D. Takeuchi, and B. Razavi, "A 10 Gb/s CMOS adaptive equalizer for backplane applications," in *IEEE Int. Solid-State Circuits Conf. Dig. Tech. Papers*, Feb. 2005, pp. 328–329.

[4] J. Lee, "A 20 Gb/s adaptive equalizer in 0.13 μm CMOS technology," in *IEEE Int. Solid-State Circuits Conf. Dig. Tech. Papers*, Feb. 2006, pp. 92–93.

[5] J. Sewter and A. C. Carusone, "A 3-tap digitally programmable transversal filter in 90 nm CMOS for equalization up to 30 Gb/s," in *IEEE Symp. VLSI Circuits Dig. Tech. Papers*, Jun. 2005, pp. 190–193.

[6] J. H. Lu, K. H. Chen, and S. I. Liu, "A 40 Gb/s low-power analog equalizer in 0.13 μm CMOS technology," in *IEEE Symp. VLSI Circuits Dig. Tech. Papers*, Jun. 2008, pp. 54–55.

[7] J. Sewter and A. C. Carusone, "A 3-tap FIR filter with cascaded distributed tap amplifiers for equalization up to 40 Gb/s in 0.18- μm CMOS," *IEEE J. Solid-State Circuits*, vol. 41, no. 8, pp. 1919–1929, Aug. 2006.

[8] G. Zhang, P. Chaudhari, and M. M. Green, "A BiCMOS 10 Gb/s adaptive cable equalizer," in *IEEE Int. Solid-State Circuits Conf. Dig. Tech. Papers*, Feb. 2004, pp. 482–483.

[9] A. Garg, A. C. Carusone, and S. P. Voinigescu, "A 1-tap 40-Gb/s look-ahead decision feedback equalizer in 0.18- μm SiGe BiCMOS technology," *IEEE J. Solid-State Circuits*, vol. 41, no. 10, pp. 2224–2232, Oct. 2006.

[10] S. Galal and B. Razavi, "10-Gb/s limiting amplifier and laser/modulator driver in 0.18- μm CMOS technology," *IEEE J. Solid-State Circuits*, vol. 38, no. 12, pp. 2138–2146, Dec. 2003.